MODELING DRIFT ALONG THE HELIOSPHERIC WAVY NEUTRAL SHEET

R. A. Burger
Centre for Space Research, North-West University, 2520 Potchefstroom, South Africa

ABSTRACT

Drift along the wavy heliospheric neutral sheet is believed to play an important role in cosmic-ray modulation and can explain the peaked versus flat intensity profiles during consecutive solar magnetic epochs. Modulation models are becoming more and more realistic and in order to determine the role of the wavy neutral sheet more accurately, we revisit a previous calculation for drift along it. While mathematically correct, we argue that the previous expression for neutral sheet drift, which follows naturally from the standard expression for gradient and curvature drift, must be adapted in order for the drift speed to be less than particle speed. We compare the effect of both the previous and the current more accurate version of neutral sheet drift on cosmic-ray modulation with results obtained by other methods.

Key words: cosmic rays – diffusion – magnetic fields – methods: analytical – Sun: heliosphere

1. INTRODUCTION

The drift pattern of cosmic rays that reach Earth during successive solar magnetic polarity epochs is very different within the termination shock. During the so-called $A > 0$ epochs (e.g., 1970s and 1990s), positively charged particles drift from the solar polar regions of the heliosphere toward Earth, and then out along the wavy neutral sheet. During the alternate $A < 0$ epochs (e.g., 1980s and 2000s), these particles drift along the wavy heliospheric neutral sheet toward Earth and away from it toward the solar polar regions. Since drift directions are reversed for negatively charged particles, it is common practice to refer to $qA > 0$ and $qA < 0$ epochs (here q is either positive or negative and denotes the sign of the particle's charge) during each of which drift directions are the same. What happens outside of the termination shock, inside the heliosheath (see, e.g., Florinski 2011), and beyond is at the time of writing really not clear and we will therefore consider only the region within the termination shock.

Early studies confirmed the importance of drifts (Jokipii & Levy 1977; Jokipii et al. 1977) and noted the role of drift along the wavy heliospheric neutral sheet (see, e.g., Kóta 1979; Isenberg & Jokipii 1978). Jokipii & Thomas (1981) first showed that a flat intensity profile during $qA > 0$ epochs and a peaked profile during $qA < 0$ epochs followed naturally by including a wavy neutral sheet with a varying tilt angle. This leads to an approximately 22 year cycle in cosmic-ray intensities, which is double that of the solar activity cycle. Observational results such as those of Lockwood & Webber (2005) show that for $qA < 0$, the intensity of ~1.6 GV protons at Earth increases by almost a factor of two when the tilt angle decreases from about 20° to 10° toward solar minimum. To determine whether changes in the tilt angle alone are responsible for these changes in intensity obviously requires a model for neutral sheet drift that is as accurate as possible.

The first fully three-dimensional calculation that included a wavy neutral sheet was reported by Kota & Jokipii (1982), who provided more detail of their calculations in a subsequent publication (Kóta & Jokipii 1983). Results from such earlier drift studies have since been confirmed qualitatively and in some cases quantitatively in numerous numerical modulation studies (see, e.g., Potgieter & Moraal 1985; Burger & Hattingh 1995; Hattingh & Burger 1995; Zhang 1999; Yamada et al. 1999; Florinski & Jokipii 1999; Alanko-Huotari et al. 2007; Pei et al. 2010).

Calculating gradient and curvature drift away from the neutral sheet is straightforward. A standard expression is used and the effect of turbulence on the drift coefficient was recently discussed by Burger & Visser (2010). However, when it comes to drift along the neutral sheet, a variety of techniques are used. For the case of a flat neutral sheet, Burger & Potgieter (1989) show that a boundary condition method, first implemented by Jokipii & Kopriva (1979), gives virtually identical results to the drift velocity field method of Burger et al. (1985). In two-dimensional modulation models, the effect of a wavy neutral sheet is either simulated by taking averages over a solar rotation (see, e.g., Burger & Potgieter 1989; Burger & Hattingh 1995; Hattingh & Burger 1995) or by taking into account the drift along the actual wavy neutral sheet but neglecting the azimuthal component (Caballero-Lopez & Moraal 2003; Alanko-Huotari et al. 2007). Note that Alanko-Huotari et al. (2007) carry out this procedure at all longitudes and then find an average of the radial and latitudinal components of the drift, while Caballero-Lopez & Moraal (2003) assume azimuthal symmetry. Turning now to fully three-dimensional models, Kóta & Jokipii (1983) state that they use numerical differentiation to determine drift velocities, and that this procedure gives finite drift at the neutral sheet. According to these authors, it corresponds to smearing the field transition between the grid points adjacent to the neutral sheet. This procedure seems very similar if not identical to the one described by Burger & Hattingh (1995), a conclusion borne out by the qualitative and quantitative agreement between results from these two three-dimensional codes, as illustrated in Burger & Hattingh (1995) and again in Section 4 below.

A re-evaluation of the drift field model presented by Burger & Hattingh (1995) shows that while it is mathematically correct, there is a subtlety when it comes to the magnitude of the drift speed along the wavy neutral sheet. It can become larger than particle speed, and this unintended unphysical behavior needs to be corrected. In this paper, a detailed calculation of the drift velocity field at and away from the neutral sheet is given. The starting point of this calculation is the standard expression for the drift velocity of a nearly isotropic particle distribution. We compare with results of Kóta & Jokipii (1983) and also with results from a paper by Pei et al. (2012), the latter where the drift velocity field of Burger et al. (1985) for a flat current sheet
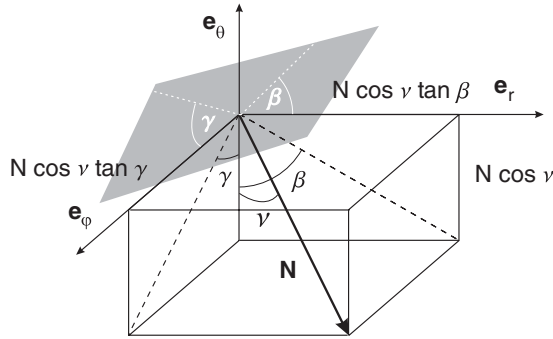
Figure 1. Vector **N**, normal to the wavy neutral sheet, and its components in terms of γ, β, and ν. Here, all three angles are positive. The gray surface is tangential to the normal, and the white dashed lines are intersections of this plane with the (θ, ϕ)-plane and the (r, θ)-plane. Note that the white dashed line in each plane is perpendicular to the black dashed line in the same plane.

is implemented in a three-dimensional modulation model. As was the case for the drift model of Burger & Hattingh (1995), the main advantage of the present model is that it requires no more computing time for a wavy neutral sheet than for a flat sheet.

A clear understanding of how to implement neutral sheet drift effectively but accurately inside the termination shock could help to address the challenge of implementing it at the same level of accuracy in the heliosheath.

2. DERIVATION OF DRIFT VELOCITY FIELD

A key assumption for the validity of the transport equation given in Section 3 is that the particle distribution is nearly isotropic, and therefore the drift velocity field must be derived for such a distribution. In this case we have that (see, e.g., Jokipii et al. 1977; Jokipii & Thomas 1981; Burger et al. 1985; Minnie et al. 2007; Burger & Visser 2010)

$$\mathbf{v}_d = -\nabla \cdot \kappa^A \equiv \nabla \times (\kappa_A \mathbf{e}_B), \tag{1}$$

where κ^A is the antisymmetric part of the diffusion tensor and κ_A is the drift coefficient. The drift velocity field is clearly divergence free and any simulation of neutral sheet drift must take this into account. The wavy neutral sheet is defined by (Kóta & Jokipii 1983)

$$\theta_{\mathrm{ns}} = \frac{\pi}{2} - \tan^{-1}(\tan \alpha \sin \phi^*), \tag{2}$$

with $\phi^* = \phi + \phi_0 + r(\Omega/V_{\mathrm{sw}})$. This expression defines the surface across which the heliospheric magnetic field, here taken to be the Parker field (Parker 1958),

$$\mathbf{B} = \frac{A}{r^2}\left(\mathbf{e}_r - \frac{r\Omega \sin \theta}{V_{\mathrm{sw}}}\mathbf{e}_\phi\right), \tag{3}$$

reverses direction as function of radial distance and azimuth. Note that while the magnitude of the magnetic field is formally zero at the neutral sheet, this is of no consequence from the point of view of the particle since it spends only an infinitesimally small time crossing it.

We now consider the geometry of the wavy neutral sheet. For a cut through it in the (r, θ)-plane, the angle β between the normal to the line tangent to the sheet and the $-\mathbf{e}_\theta$ direction (see Figure 1) follows from

$$\tan \beta = \frac{r\Delta\theta_{\mathrm{ns}}}{\Delta r}, \tag{4}$$

where $r\Delta\theta_{\mathrm{ns}}$ is the infinitesimal change in the θ-direction as r changes by Δr. Note that $-\pi/2 < \beta < \pi/2$. Similarly, we find that in the (θ, ϕ)-plane (see Figure 1)

$$\tan \gamma = \frac{r\Delta\theta_{\mathrm{ns}}}{r \sin \theta \Delta\phi}, \tag{5}$$

and again $-\pi/2 < \gamma < \pi/2$. For the wavy neutral sheet defined in Equation (2), it then follows that

$$\tan \beta = \frac{r\partial\theta_{\mathrm{ns}}}{\partial r} = -\frac{r\frac{\Omega}{V_{\mathrm{sw}}}\tan \alpha \cos \phi^*}{1 + \tan^2\alpha\sin^2\phi^*} \tag{6}$$

and

$$\tan \gamma = \frac{r\partial\theta_{\mathrm{ns}}}{r \sin \theta \, \partial\phi} = -\frac{\tan \alpha \cos \phi^*}{\sin \theta(1 + \tan^2\alpha\sin^2\phi^*)}. \tag{7}$$

From Equation (6), we find that

$$\cos \beta = \left[1 + \left(\frac{r\frac{\Omega}{V_{\mathrm{sw}}}\tan \alpha \cos \phi^*}{1 + \tan^2\alpha\sin^2\phi^*}\right)^2\right]^{-1/2} \tag{8}$$

in agreement with the corresponding expression given by Caballero-Lopez & Moraal (2003) if the tilt angle is sufficiently small so that $\tan \alpha \approx \alpha \ll 1$. Note that the expression for the wavy neutral sheet used by these authors is different from the more generally valid one in Equation (2).

For a Parker field, the angles β and γ are related through

$$\frac{\tan \beta}{\tan \gamma} = r \sin \theta \frac{\Omega}{V_{\mathrm{sw}}} \equiv \tan \Psi, \tag{9}$$

with Ψ the winding angle.

The tangent of the angle ν between the normal **N** to the sheet and the $-\mathbf{e}_\theta$-direction readily follows from Figure 1 as

$$\tan \nu = \pm\sqrt{\tan^2\beta + \tan^2\gamma} = \frac{\tan \beta}{\sin \Psi} \tag{10}$$

or

$$\cos \nu = (1 + \tan^2\beta + \tan^2\gamma)^{-1/2}. \tag{11}$$

As was the case for β and γ, $-\pi/2 < \nu < \pi/2$, and all three angles have the same sign.

To model the presence of a wavy neutral sheet in a numerical modulation model, we now multiply κ_A in Equation (1) with a transition function, so that

$$\kappa_A \rightarrow \kappa_A \tanh\left[k\left(\theta_{\mathrm{ns}} - \theta\right)\cos \nu\right]. \tag{12}$$

This procedure ensures that the global drift velocity field remains divergence free. Note however that the terms that follow from it are not necessarily divergence free when considered individually. The hyperbolic tangent models the reversal in the magnetic field direction across the neutral sheet, and the $\cos \nu$ adjusts the width of the meridional region over which neutral sheet drift is modeled. Since $\cos \nu$ is closest to 1 near the crests and troughs of the neutral sheet, its effect there is negligible. However, its minimum values occur where the neutral sheet crosses the ecliptic plane, and there its effect is the largest, increasing the angular distance over which neutral sheet drift is modeled.

The drift velocity from Equation (1) with κ_A redefined as in Equation (12) is then

$$\mathbf{v}_d = (\nabla \times \kappa_A \mathbf{e}_B) \tanh\left[k\left(\theta_{\mathrm{ns}} - \theta\right)\cos \nu\right]$$
$$- \frac{k \cos \nu}{\cosh^2\left[k\left(\theta_{\mathrm{ns}} - \theta\right)\cos \nu\right]} \kappa_A \mathbf{e}_B \times \nabla(\theta_{\mathrm{ns}} - \theta)$$
$$- \frac{k(\theta_{\mathrm{ns}} - \theta)}{\cosh^2\left[k\left(\theta_{\mathrm{ns}} - \theta\right)\cos \nu\right]} \kappa_A \mathbf{e}_B \times \nabla \cos \nu. \quad (13)$$

The first term, which is zero at the neutral sheet, represents gradient and curvature drift away from the sheet, while the second term (denoted by $\mathbf{v}_{\mathrm{dns}}$ in what follows) represents neutral sheet drift. The third term on the right-hand side, which is zero at the current sheet, depends on the gradient of the $\cos \nu$ term. It turns out that the cross product has a θ-component only, and this component alternates between the positive and negative values. Differences between the absolute values of the positive and negative peaks are most pronounced in the inner heliosphere but become negligible beyond about 10 AU. This drift therefore moves particles up and down in latitude but does not contribute significantly to the drift flux in a realistic-sized heliosphere. It is therefore neglected.

Because the reversal in the magnetic field direction across the neutral sheet is now modeled by the hyperbolic tangent function, the unit vector $\mathbf{e}_B$ is *always* that for $A > 0$ in the Northern hemisphere of the heliosphere. (If either the magnetic polarity changes to $A < 0$ or the particles are negatively charged, all drift directions reverse.) Therefore

$$\mathbf{e}_B = \cos \Psi \mathbf{e}_r - \sin \Psi \mathbf{e}_\phi, \quad (14)$$

and by calculating

$$\nabla(\theta_{\mathrm{ns}} - \theta) \equiv \frac{\partial \theta_{ns}}{\partial r} \mathbf{e}_r - \frac{1}{r} \mathbf{e}_\theta + \frac{1}{r \sin \theta} \frac{\partial \theta_{ns}}{\partial \phi} \mathbf{e}_\phi \quad (15)$$

using Equation (2), it follows that the second term of Equation (13) becomes

$$\mathbf{v}_{\mathrm{dns}} = \frac{k}{r \cosh^2\left[k\left(\theta_{\mathrm{ns}} - \theta\right)\cos \nu\right]} \kappa_A \mathbf{e}_{\mathrm{ns}} \quad (16)$$

with the unit vector in the direction of neutral sheet drift given by

$$\mathbf{e}_{\mathrm{ns}} = \sin \Psi \cos \nu \, \mathbf{e}_r + \sin \nu \, \mathbf{e}_\theta + \cos \Psi \cos \nu \, \mathbf{e}_\phi. \quad (17)$$

Without the $\cos \nu$ in the transition function in Equation (12), a $\cos \nu$ would still appear in the denominator of Equation (16) but now multiplying the hyperbolic cosine term and not as part of its argument. This is of no consequence for a flat sheet for which $\cos \nu = 1$, but as the tilt angle increases and $\cos \nu$ becomes smaller than 1, the neutral sheet drift speed can become much larger than the particle speed in a rather narrow region. This leads to unphysically large drift speed gradients and consequently instabilities when solving the Parker transport equation on a finite grid using the alternating direction implicit technique.

For completeness, we note that in the code we set the parameter $k = 27.52 \, P^{-0.25}$ if $P > 3.5$ GV, and $k = 20.12$ if $P \leqslant 3.5$ GV. This ensures that the angular width over which neutral sheet drift is assumed to occur for $\cos \nu = 1$ is equivalent to two gyroradii at 16 GV ($\sim 11{.}7$) and constant at $\sim 6°$ below 3.5 GV. This means that in our code the neutral sheet drift profile is distributed over at least four grid points on either side

of the wavy neutral sheet. Although the drift velocity field is divergence free for any choice of k, its actual value is not totally free. One should keep in mind that gradient and curvature drift that occurs away from the neutral sheet is also affected by the choice of k through the hyperbolic tangent function in the first term of Equation (13). If k is too small and the angular width over which the modeled neutral sheet drift occurs therefore too large, the region over which gradient and curvature drift operates and moves particles either toward or away from the neutral sheet becomes too small. When this happens, drift effects are reduced and intensities can approach no-drift values. If, on the other hand, k is too large, the neutral sheet drift profile will not be properly sampled in a numerical code that solves the cosmic-ray transport equation on a grid; its effect will either be over-estimated or the code can become unstable, as discussed above.

3. MODULATION MODEL

We have set up our modulation model to be as close as possible to the one described in Kota & Jokipii (1982) and Kóta & Jokipii (1983). We also solve Parker's transport equation (Parker 1965) in a frame corotating with the Sun and in which structures such as the wavy neutral sheet are static. Time dependence is eliminated from Parker's equation through

$$\frac{\partial f}{\partial t} + (\mathbf{\Omega} \times \mathbf{r}) \cdot \nabla f = 0, \quad (18)$$

which leads to

$$\nabla \cdot (\mathsf{K}^S \cdot \nabla f) - (\mathbf{v}_d + \mathbf{V}^*) \cdot \nabla f + \tfrac{1}{3}(\nabla \cdot \mathbf{V}^*)\frac{\partial f}{\partial \ln p} = 0. \quad (19)$$

Here $\mathbf{V}^* = \mathbf{V}_{\mathrm{sw}} - \mathbf{\Omega} \times \mathbf{r}$ with $\mathbf{V}_{\mathrm{sw}}$ the solar wind velocity, $\mathbf{\Omega}$ is the solar rotational velocity, $\mathbf{v}_d$ is the drift velocity, with $\mathbf{r}$ the position and p the momentum of the cosmic rays, and K^S is the symmetric part of the diffusion tensor. The distribution function f is related to the differential intensity with respect to kinetic energy, j_T, by $j_T = p^2 f$.

The solar wind speed is taken as 400 km s^{-1} and the outer boundary is set at 10 AU where a local interstellar spectrum (LIS) is specified, given by

$$j_T^{\mathrm{LIS}} = 10\beta \, P^{-2.6} \quad (20)$$

in units of particles m^{-2} s^{-1} sr^{-1} MeV^{-1}. Here, P is particle rigidity and β is the ratio of particle speed to the speed of light. The functional form is equivalent to that of the distribution function given in Kóta & Jokipii (1983).

The parallel- and perpendicular-diffusion coefficients and the drift coefficient as given in Kóta & Jokipii (1983) are

$$\kappa_{||} = \kappa_0 \beta \, P^{1/2} \frac{B_{\mathrm{Earth}}}{B} \quad (21)$$

$$\kappa_{\perp} = 0.05 \kappa_{||} \quad (22)$$

$$\mathrm{and} \quad \kappa_A = \frac{pv}{3qB} \quad (23)$$

with v the particle speed, q the particle charge, $\kappa_0 = 5 \times 10^{21}$ cm^2 s^{-1}, and B the magnitude of the Parker field (3), with B_{Earth} its magnitude at Earth, taken to be 5 nT.
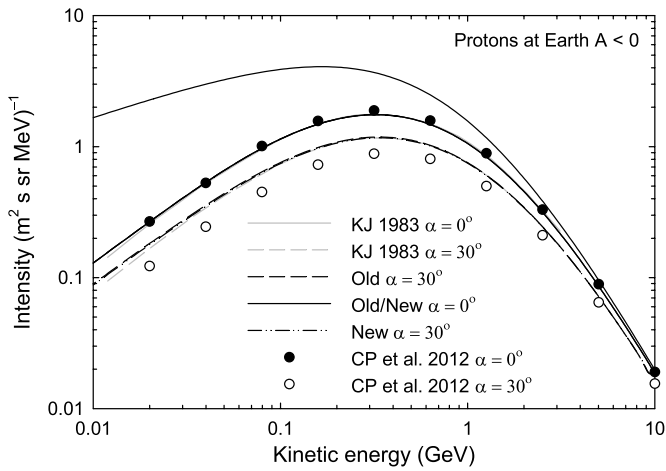
Figure 2. Proton spectra at 1 AU for $A < 0$ and for tilt angles 0° and 30°. "KJ 1983" denotes the results of Kóta & Jokipii (1983), "New" denotes results with the drift velocity field (16), "Old" denotes results when the transition function in Equation (12) is used without the $\cos \nu$ term, and "CP et al. 2012" denotes results from Pei et al. (2012). Note that the solutions for $A > 0$ for Old and New are identical.

4. MODEL RESULTS AND COMPARISONS

In what follows, we refer to Equation (16) as the new drift velocity field, and the same equation but with $\cos \nu$ in the denominator multiplying the hyperbolic cosine and not as part of its argument, i.e., using the transition function in Equation (12) without the $\cos \nu$ term, as the old drift velocity field, as used by, e.g., Burger & Hattingh (1995).

The agreement in Figure 2 between the 1 AU spectra calculated using the old drift velocity field (black solid line) and the new one for $\alpha = 0°$ is exact as one would expect, because in this case $\cos \nu = 1$. When $\alpha = 30°$, the agreement between the old drift velocity field (black dashed line) and the new one (black dash-dot-dot line) is very good with differences of less than 2%. Moreover, the agreement with the results of Kóta & Jokipii (1983) for both $\alpha = 0°$ (gray solid line) and $\alpha = 30°$ (gray dashed line) is also very good except at the lowest energies. This difference may be an artifact of the way Kóta & Jokipii (1983) plotted their results; their spectra do not show the adiabatic limit where the intensity becomes proportional to kinetic energy, as is the case for the spectra from the current study. We note that if our neglect of the third term in Equation (13) had significant consequences, we would have expected it to show up in this comparison with a small heliosphere. While the spectrum of Pei et al. (2012) agrees very well with the other two for $\alpha = 0°$ (solid circles), it is clearly different from both for $\alpha = 30°$ (open circles).

In Figure 3, the intensity-tilt curves of 1.6 GeV protons at Earth for the old- and the new-drift velocity field for $A > 0$ (black dashed lines) are identical, and less than 2% higher than the result of Kóta & Jokipii (1983) (gray dashed line) at small tilt angles where the difference is at its largest. For $A < 0$, the old- (black solid line) and the new-drift (black dash-dot-dot line) velocity field differ by less than 1% at this energy. While the value of Kóta & Jokipii (1983) appears to be some 5% higher at $\alpha = 0°$, we note that when this value is calculated directly from the spectra given by these authors, it is about 2% lower than the value found in the present study. Similarly, the value at $\alpha = 30°$ may actually be some 4% lower than the value found in the present study. However, even taking into account these ambiguities, the intensity-tilt curves for both the old- and the
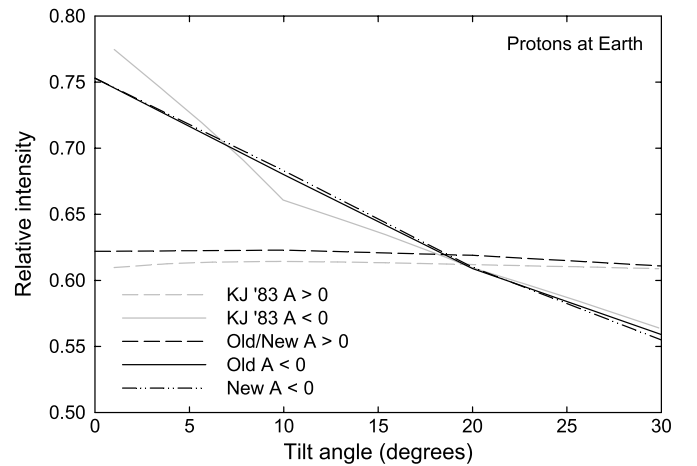

Figure 3. Intensity of 1.6 GeV protons at Earth, normalized with respect to the LIS, as a function of tilt angle. Legend for the different lines is the same as for Figure 2.

new-drift field agree quite well with the results of Kóta & Jokipii (1983).

Figure 4 shows intensity contours of 1.6 GeV protons at 1 AU for a tilt angle of 30°, for both magnetic polarity epochs, produced with the new drift velocity field. This figure shows good agreement with the corresponding Figure 1 of Kóta & Jokipii (1983).

5. SUMMARY AND CONCLUSIONS

We present a new three-dimensional drift velocity field that includes the effect of a wavy neutral sheet in a very simple manner. The derivation follows that of Burger & Hattingh (1995) which has the standard expression for drift of a nearly isotropic distribution of particles as its starting point and is mathematically correct, but yields a drift speed along the wavy neutral sheet that can exceed particle speed. The problem is similar to that of the δ-function concept of neutral sheet drift for a flat sheet, a result that must be reinterpreted for it to make physical sense (see, e.g., Isenberg & Jokipii 1979; Burger 1987). This new and more accurate neutral sheet drift velocity field model yields results that agree very well with that of Kóta & Jokipii (1983), calculated for a small heliosphere. Runs performed thus far show that when a more realistic size for the heliosphere is used so that $\cos \nu$ becomes sufficiently small, the old model causes instabilities while the new model does not. This was also verified with an ab initio code under construction (E. Engelbrecht 2012, private communication). It seems that while the code remains stable, the results for the old- and the new-drift velocity field model do not differ hugely. As an example, when the code is run for a 40 AU heliosphere with tilt angles up to 40° but with the same parameters as in Kóta & Jokipii (1983), an intensity-tilt comparison shows that the old model gives higher intensities than the new one, varying from 3% at 10° tilt for 1.6 GeV protons at Earth for $A < 0$ to 13% at 30° tilt; at 40° tilt the old model goes unstable but the new one does not. The higher intensities for the old model are to be expected because the neutral sheet drift speeds are larger and the effect of the neutral sheet is therefore reduced. For $A > 0$ the models give virtually identical result up to a tilt angle of 30°, but the old one again goes unstable when the tilt angle is at 40°.

A key advantage of the method described in this paper is that it requires no more computing time for a wavy neutral sheet
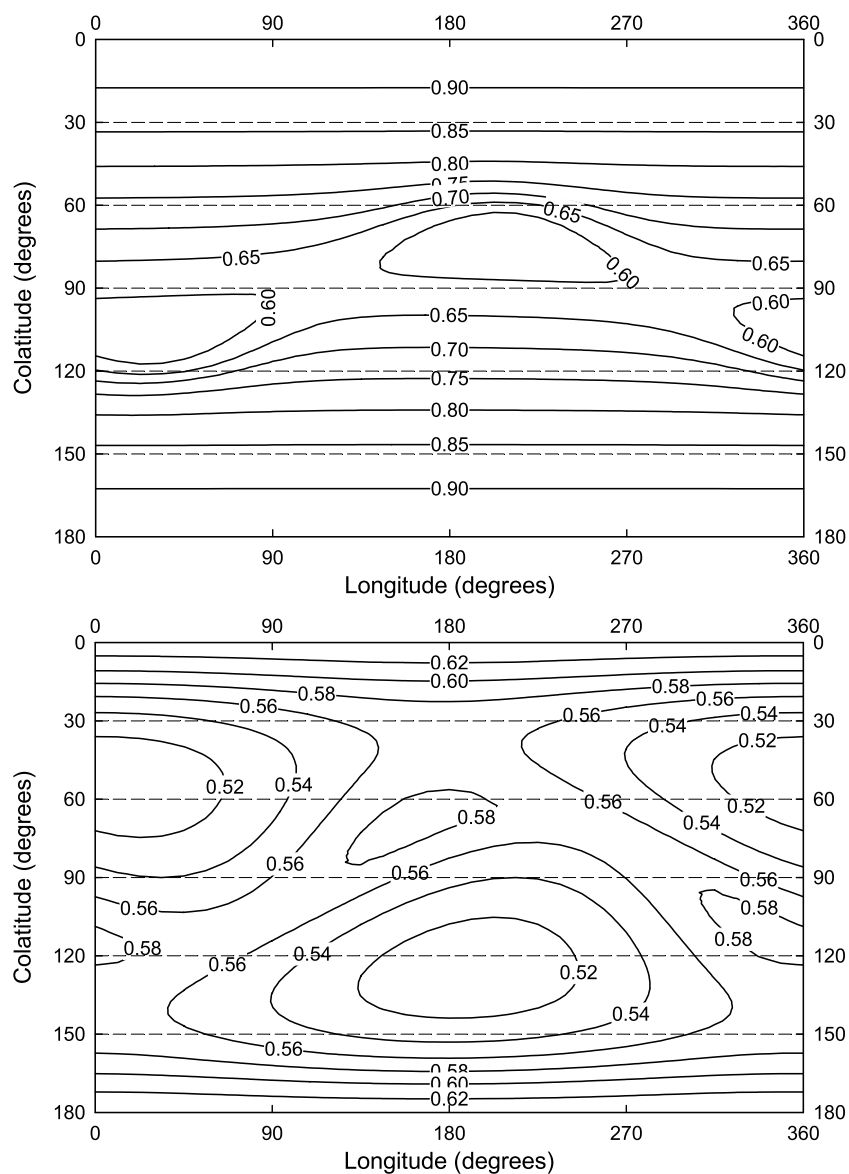
Figure 4. Intensity contours of 1.6 GeV protons at 1 AU for a tilt angle of $30°$, for $A > 0$ (top panel) and $A < 0$ (bottom panel).

REFERENCES

Alanko-Huotari, K., Usoskin, I. G., Mursula, K., & Kovaltsov, G. A. 2007, J. Geophys. Res. (Space Phys.), 112, 8101
Burger, R. A. 1987, PhD thesis, Potchefstroomse Universiteit vir Christelike Hoër Onderwys
Burger, R. A., & Hattingh, M. 1995, Ap&SS, 230, 375
Burger, R. A., Moraal, H., & Webb, G. M. 1985, Ap&SS, 116, 107
Burger, R. A., & Potgieter, M. S. 1989, ApJ, 339, 501
Burger, R. A., & Visser, D. J. 2010, ApJ, 725, 1366
Caballero-Lopez, R. A., & Moraal, H. 2003, in Proc. 28th International Cosmic Ray Conf., Vol. 7, ed. A. K. Y. M. T. Kajita, Y. Asaoka, & M. Sasaki (Tokyo: Universal Academy Press, Inc.), 3871
Florinski, V. 2011, Adv. Space Res., 48, 308
Florinski, V., & Jokipii, J. R. 1999, ApJ, 523, L185
Hattingh, M., & Burger, R. A. 1995, Adv. Space Res., 16, 213
Isenberg, P. A., & Jokipii, J. R. 1978, ApJ, 219, 740
Isenberg, P. A., & Jokipii, J. R. 1979, ApJ, 234, 746
Jokipii, J. R., & Kopriva, D. A. 1979, ApJ, 234, 384
Jokipii, J. R., & Levy, E. H. 1977, ApJ, 213, L85
Jokipii, J. R., Levy, E. H., & Hubbard, W. B. 1977, ApJ, 213, 861
Jokipii, J. R., & Thomas, B. 1981, ApJ, 243, 1115
Kóta, J. 1979, in Proc. 16th International Cosmic Ray Conf., Vol. 3, ed. S. Miyake (Tokyo: Institute for Cosmic Ray Research, University of Tokyo), 13
Kota, J., & Jokipii, J. R. 1982, Geophys. Res. Lett., 9, 656
Kóta, J., & Jokipii, J. R. 1983, ApJ, 265, 573
Lockwood, J. A., & Webber, W. R. 2005, J. Geophys. Res. (Space Phys.), 110, 4102
Minnie, J., Bieber, J. W., Matthaeus, W. H., & Burger, R. A. 2007, ApJ, 670, 1149
Parker, E. N. 1958, ApJ, 128, 664
Parker, E. N. 1965, Planet. Space Sci., 13, 9
Pei, C., Bieber, J. W., Burger, R. A., & Clem, J. 2010, J. Geophys. Res. (Space Phys.), 115, 12107
Pei, C., Bieber, J. W., Burger, R. A., & Clem, J. 2012, ApJ, 744, 170
Potgieter, M. S., & Moraal, H. 1985, ApJ, 294, 425
Yamada, Y., Yanagita, S., & Yoshida, T. 1999, Adv. Space Res., 23, 505
Zhang, M. 1999, ApJ, 513, 409